Cardiomyocyte-specific overexpression of estrogen receptor beta improves survival and cardiac function after myocardial infarction in female and male mice

Iris Schuster[1]*, Shokoufeh Mahmoodzadeh[2,4]*, Elke Dworatzek[3,4]*, Frédéric Jaisser[5], Smail Messaoudi[5], Ingo Morano[2], and Vera Regitz-Zagrosek[3,4]

[1]EA 2992, Medical University of Nîmes-Montpellier, Centre Hospitalo-Universitaire de Nîmes, France; [2]Max-Delbrueck-Center for Molecular Medicine in the Helmholtz Association, Berlin, Germany; [3]Institute of Gender in Medicine and Center for Cardiovascular Research, Charité Universitaetsmedizin Berlin, Germany; [4]DZHK (German Center for Cardiovascular Research), partner site Berlin, Berlin, Germany, [5]Inserm, U872, Paris, France

*Authors contributed equally to this work.

Total word count: 4698

Corresponding author:
Elke Dworatzek, PhD
Charité Universitaetsmedizin
Institute of Gender in Medicine and Center for Cardiovascular Research
Hessische Strasse 3-4
10115 Berlin, Germany
Phone: +49-30-450 525 287
Fax: +49-30-450 525 943
E-mail: Elke.Dworatzek@charite.de

Abstract

Background: Estrogen receptor beta (ERβ) activation has been shown to be cardioprotective, but the involved cell types and mechanisms are not understood. To investigate whether ERβ restricted to cardiomyocytes contributes to observed cardioprotection, we tested the effects of a cardiomyocyte-specific ERβ overexpression (ERβ-OE) on survival, cardiac remodelling and function after myocardial infarction (MI) and studied potentially involved molecular pathways.

Methods and Results: Female and male mice with cardiomyocyte-specific ERβ-OE and wild type (WT) littermates were subjected to chronic anterior coronary artery ligation or sham surgery. Two weeks after MI, ERβ-OE mice showed improved survival (100 and 83% vs 76 and 58% in WT females and males respectively). ERβ-OE was associated with attenuated left ventricular (LV) dilatation, smaller increase in heart weight, less lung congestion at similar MI size, and improved systolic and diastolic function in both sexes. We identified two potential pathways for ERβ mediated myocardial protection. First, male and female ERβ-OE mice had a lower reduction of SERCA2a expression after MI, suggesting less reduction in diastolic Ca^{2+}-reuptake into sarcoplasmic reticulum post MI. Second, male ERβ-OE revealed attenuated cardiac fibrosis in the remote LV tissue and expression of fibrosis markers *Col I, Col III*, periostin, and miR21.

Conclusions: Cardiomyocyte-specific ERβ-OE improved survival associated with reduced maladaptive remodelling, improved cardiac function and less heart failure development after MI in both sexes. These effects seem to be related, at least in part, to a better maintenance of Ca^{2+}-cycling in both sexes and a lower induction of cardiac fibrosis in males after MI.

Summary statement: The study provides new insights into cardiomyocyte-specific effects of ERβ in the setting of chronic MI using a transgenic mouse model. ERβ-OE mice of both sexes showed improved survival, less maladaptive LV remodelling, better cardiac function and less HF development.

Short title: Effects of ERβ overexpression after MI

Key words: estrogen receptor beta, myocardial infarction, cardiac function, fibrosis, sex

Abbreviations list

AKT1/2/3	Serin/Threonin-kinase (protein kinase B)
Col I	Collagen I
Col III	Collagen III
DAPI	6-diamidino-2-phenylindole
E/E'	Ratio of early mitral velocity to early diastolic velocity of the mitral annulus
EF	Ejection fraction
ERK1/2/p-ERK1/2	Extracellular regulated kinase 1/2/ phospho-extracellular regulated kinase 1/2
ERα/β	Estrogen receptor alpha/beta
ERβ-OE	Estrogen receptor beta over-expression
GAPDH	Glyceraldehyd-3-phosphate dehydrogenase
HF	Heart failure
LV	Left ventricle
LVEDV	Left ventricular enddiastolic volumes
LVESV	Left ventricular endsystolic volumes
MI	Myocardial infarction
miR	Micro RNA
Myh 6/7	Myosin heavy chain 6/7
NPPA	Atrial natriuretic peptide A
PI3K	Phosphatidylinositol-4,5-bisphosphate 3-kinase
PLN	Phospholamban
RPLO	50S ribosomal protein L15
SERCA2a	Sarcoplasmic/endoplasmic reticulum calcium ATPase 2
SR	Sarcoplasmic reticulum
TDI	Tissue Doppler imaging
WT	Wild type

Introduction

Sex has an important impact on cardiac remodelling, which is defined as changes in structure, dimensions and physiology of the heart after injury [1]. In response to myocardial infarction (MI), women experience less adverse left ventricular (LV) remodelling than men, resulting in better preservation of LV size and function [2, 3]. In animal models of MI, female mice showed improved survival, maladaptive remodelling and cardiac function compared to males [4]. These differences between sexes have been widely related to the sex hormone estrogen. Estrogen-effects are mainly mediated by two cognate receptors, ERα and ERβ, which are expressed in the myocardium of males and females in a broad variety of species ranging from mice to human [5-8]. Albeit both ER subtypes activate a variety of signal transduction pathways [9, 10], functions of the individual ER subtypes are still not completely understood. The development of transgenic and knock-out animal models has helped so far to elucidate this important issue.

Studies using mouse models to analyze the role of ER in MI pointed to a protective role of ERβ in female mice. Pelzer *et al.* [11] showed increased mortality and aggravated clinical and biochemical markers of heart failure (HF) in systemic ERβ knock-out (ERβ$^{-/-}$) female mice after experimental MI. Korte *et al.* [12] observed impaired repolarization and automaticity in female mice post-MI, and Babiker *et al.* [13] observed increased MI size among female ERβ$^{-/-}$ mice.

The molecular basis for the observed cardioprotective effects of ERβ after MI needs further investigation. Pelzer *et al.* observed an impairment of calcium-handling proteins in female ERβ$^{-/-}$ mice [11]. In a model of pressure overload using systemic ERβ knock-out (ERβ$^{-/-}$) mice, we recently showed that ERβ attenuates the development of LV fibrosis [14].

Furthermore, activation of specific myocardial hypertrophy associated signalling pathways has been shown to be cardioprotective [15]. For instance, increased PI3-K–AKT activity led to improved survival in a mouse model of dilated cardiomyopathy and to favourable effects on cardiac function and remodeling [16, 17]. We and others showed that cardioprotective signalling pathways are modulated by ERβ [18, 19].

The effects of ERβ in the male sex after MI have not been studied yet. Furthermore, using systemic knock out models, it has not been clarified whether systemic or cardiac specific effects of ERβ confer cardioprotection. In the present study, we therefore used a cardiomyocyte-specific ERβ overexpression (ERβ-OE) mouse model which allowed the analysis of cardiac effects of ERβ independently of systemic effects on both sexes subjected to MI. The main hypothesis of this study was that a cardiomyocyte-specific ERβ-OE attenuates pathological myocardial remodelling and preserves cardiac function after MI in both sexes.

Materials and Methods

Generation of transgenic mice

A novel transgenic mouse model with cardiomyocyte-specific ERβ-OE was generated. Inducible double transgenic mice with cardiomyocyte-specific ERβ-OE were generated through mating of monotransgenic mouse ERβ (tetO-mERβ) and monotransgenic β-MHC-tTA mice using Tet-Off system (details online supplement). Male and female ERβ-OE and WT mice with B6D2F background were used.

Induction of myocardial infarction

Experiments were conducted in accordance with the Guide for the Care and Use of Laboratory Animals published by the US National Institutes of Health (NIH Publication No. 85-23, revised 2011) and with the guidelines of the State Agency for Health and Social Affairs (LaGeSo, Berlin, Germany, G0246/12). Female and male ERβ-OE and WT littermates aged 10-12 weeks, were randomly assigned to MI or sham surgery. MI was induced in female and male mice by permanent left anterior descending coronary artery ligation. Briefly, after induction of anesthesia (ketamine hydrochloride 80mg/ml and xylazine hydrochloride 12mg/ml by intraperitoneal injection at a dose of 1mg/kg), mice were intubated and ventilated (respirator: Hugo Basile model; FMI). After exposing the left anterior descending coronary artery through a 4th intracostal left lateral thoracotomy, the artery was permanently ligated with a 7.0 polypropylene suture at a distance of 1–2 mm from the left auricle. Sham animals underwent the same surgical procedure but the ligature was not tied. Animals were treated with rimadyl (5mg/kg) for analgesia up to 7 days post-surgery.

High resolution echocardiography

Echocardiography was performed under isoflurane anesthesia one day before and 2 weeks after surgery with a Vevo 770 (VisualSonics, Toronto, Canada) [14] equipped with a 20-55 MHz transducer. Anaesthesia was induced with isoflurane 3% and maintained with isoflurane 1.5%. Body temperature was maintained through a heating pad at 37°C. Electrocardiogram and respiration were monitored during echocardiography. Images and cineloops were acquired for further off-line analysis by a single operator blinded for genotype, sex and operation. LV enddiastolic and endsystolic volumes (LVEDV, LVESV), mean wall thickness, and ejection fraction (EF) were determined by tracing of endocardial and epicardial borders and majors in enddiastole and in endsystole in the parasternal long axis view. Transmitral flow-analysis from the four chamber view was used to characterize diastolic function from the following parameters: peak E and A waves, E wave deceleration time and filling interval. Pulsed-wave Doppler measurements were made at the ascending aorta level for the determination of ejection time and LV pre-ejection time, and at the origin of the pulmonary artery for the determination of right ventricular pre-ejection time. The difference between the electromechanical ejection delay of the LV (duration from the QRS complex to the beginning of the aortic outflow) and of the right ventricular (duration from de QRS complex to the beginning of the pulmonary outflow) was used as an index of interventricular asynchrony [20]. Tissue Doppler imaging (TDI) systolic S and diastolic E' wave from the septal side of the mitral annulus were measured and the ratio transmitral E to mitral annulus E' was calculated. The myocardial performance index [(filling interval – ejection time)/ejection time] was calculated as an index of global systolic and diastolic function.

Infarct size determination

MI size was determined by echocardiography based on LV wall motion according to the method used in clinical routine in humans [21]. Since the development of high resolution ultrasound machines, echocardiographic analysis is recognized as a precise and non-invasive evaluation technique for LV morphology and function in small animals [22, 23]. An additional advantage is the preservation of LV tissue for molecular analysis in the same cohort of animals. Echocardiographic evaluation of MI size has been shown to strongly correlate with histologic determination (r=0.96) [24] and with LV systolic dysfunction (r=0.94) [25]. We used the Electrocardiogram-Gated Kilohertz Visualization™-mode which

synthesizes high temporal resolution B-Mode images by combining Electrocardiogram-synchronized heart cycles, thus producing sequences at up to 1000 frames per second. The synthesized cycle was displayed in slow motion before tracing endocardial perimeters at enddiastole. As shown in Fig. 1A, MI size was determined from the long axis view obtained with a high definition in mice. MI size (%) was calculated [24] as the internal perimeter of the infarcted region, identified by a thinned akinetic wall, in relation to the total perimeter of the LV cavity: MI (%) = MI perimeter/(MI perimeter + normal endocardial perimeter)x100. For comparison, MI size was also determined as the mean from 4 different short axis views at basal, papillary, mid-ventricular and apical LV level (Fig. 1B) which show horizontal views of the ventricle. Fig. 1C shows a high correlation between MI size determined from long and short axis views (r^2 = 0.94; p<0.0001, n=67). As small infarcts induce no global or only minimal regional remodeling, only animals with an MI size > 20% in the MI groups were included.

Tissue sampling
Mice that died before the end of the observation period were subjected to autopsy, and heart and lungs were examined. Two weeks after MI, surviving mice were anesthetized with isoflurane (1.5%) and killed by cervical dislocation. Hearts were harvested, LV isolated, immediately snap frozen in liquid nitrogen and stored at -80°C or fixed in 4% formaldehyde for at least 24h; until use for gene and protein or histological analyses.

Cell morphology
Adult mouse ventricular cardiomyocytes were isolated as described previously [26]. Individual length and width of the cardiomyocytes were determined on micrographs captured by Axiovert 40 CFL microscope (using objective: N-Achroplan 10x/0.25 Ph1 W 0.8) and digitalized by AcioCam MR3 camera. Ten micrographs per sample were randomly taken, and 300 to 500 rod-shaped myocytes were measured per sex and genotype. Length and width of cardiomyocytes were determined at the widest point of each cell using the software program "AxioVision Release 4.8" (Zeiss).

Quantitative real-time polymerase chain reaction
Total RNA isolation from LV tissue and quantitative real-time polymerase chain reaction were conducted as described before [18, 14]. The primers used for quantification of relative gene expression of mouse collagen I and III (*Col1A2*, *Col3A1*), atrial natriuretic peptide A (*NPPA),* myosin heavy chain *(Myh)* 6, *Myh*7, microRNA (miR)-21, miR-24, miR-27a, miR-106a are listed in supplemental table 1. Gene expression levels were normalized to 50S ribosomal protein L15 (*RPLO*) and the amount of miRNAs was normalized using the average of the expression of RNU6B and RNU1A.

Western blot analysis
Analysis was performed as described before [6]. The following primary antibodies were used: ERα (G-20, Santa Cruz); ERβ (SP5198P, Acris); periostin (S-15, Santa Cruz); sarcoplasmic/endoplasmic reticulum calcium ATPase 2 (ATP2A2/SERCA2a, SM5113, Acris); phospholamban (PLN, SAB2701037, Sigma-Aldrich); phospho-phospholamban (p-PLN, sc-17024-R, Santa Cruz); phospho-p44/p42 ERK1/2 (Thr202/Tyr204) (#4370, Cell Signaling Technology); p44/p42 ERK1/2 (#4695, Cell Signaling Technology); phospho-Serin/Threonin-kinase (AKT1/2/3) (Ser 473-R, Santa Cruz); AKT1/2/3 (H-136, Santa Cruz); α-tubulin (clone DM1A, Sigma) and GAPDH (MAB374, Millipore).

Histological analysis and Immunofluorescence
LV sections were stained with Sirius-red to determine collagen deposition as previously described [18]. Fibrosis in remote area was calculated as the ratio of fibrotic area (excluding the MI zone) to total myocardial area in the remote zone. For immunofluorescence, paraffin-embedded sections were incubated with anti-mouse ERβ antibody (Acris SP5198P) followed by secondary Fluorescein isothiocyanate-conjugated anti-mouse IgG (Jackson ImmunoResearch Laboratories), as described before [7]. Nuclei were stained with 6-

6

diamidino-2-phenylindole (DAPI). Confocal images were acquired using Leica TCS-SPE spectral confocal laser scanning microscope.

Statistical analysis

Data are shown as mean ± standard error of the mean (SEM). The differences between groups were tested by using ANOVA as appropriate. Three-way ANOVA was used to analyze interactions between operation, genotype and sex, followed by PLSD Fisher post-test to independently assess the overall effect of operation (MI vs sham), genotype (ERβ-OE vs WT) or sex (male vs female). Two-way ANOVA was used to test the influence of operation independent of genotype, and of genotype independent of sex, followed by Bonferroni post hoc test using GraphPad Prism 5.01. MI Mortality was illustrated by Kaplan-Meier curves and analysed by log-rank test. Peri-procedural deaths within the first 24 hours after the operation were excluded. P≤0.05 were considered statistically significant.

7

Results

Characterization of ERβ-OE mice

There were no differences in heart weight, LV morphology, cardiac function (supplemental table 2) and cardiomyocyte size (Fig. 2A) between ERβ-OE and WT mice at basal level. ERβ protein was significantly higher in whole protein lysate from LV of ERβ-OE compared to WT mice (female: 1.8 fold and male: 1.5 fold; Fig. 2B). ERβ-OE in the LV was confirmed by immuno-fluorescence (Fig. 2C). ERβ-OE was specific to the heart, and ERβ expression did not increase in kidney, soleus and uterus of ERβ-OE mice (supplemental Fig. 1). There was no change of ERα protein expression in LV tissues (Fig. 2D). Blood serum estradiol levels were not different between ERβ-OE and WT mice (supplemental results).

ERβ-OE reduces mortality rate after myocardial infarction

ERβ-OE significantly reduced mortality compared to WT mice after MI (Fig. 3; p=0.008). The survival rate 2 weeks after MI was 100 and 83% in ERβ-OE, and 76 and 58% in WT female and male mice, respectively. Female and male WT mice that died before the end of the observation period showed 25 and 50% of cardiac rupture respectively, with a peak at day 3.8±0.8, whereas no rupture was observed in ERβ-OE mice. Cardiac rupture was indicated by blood coagula in the chest cavity and small slits commonly observed at the LV free wall. After day 4, only female and male WT mice died, showing signs of pulmonary congestion at autopsy.

ERβ-OE attenuates LV maladaptive remodelling

After MI, LV mean wall thickness was reduced due to the thinned infarcted myocardial wall, whereas LV volumes increased (table 1). ERβ-OE did not affect MI size, but was associated with reduced LV maladaptive dilatation. ERβ-OE mice had a smaller increase of LVEDV and LVESV with a sex-genotype-surgery interaction for both parameters after MI (table 1). ERβ-OE was also associated with a smaller increase in heart and lung weight normalized for tibia length with a genotype-surgery interaction. WT mice had not only higher heart but also higher lung weight, indicating a more advanced stage of HF compared to ERβ-OE. Separate analysis in each sex after MI showed a significant ERβ-OE effect on LV volumes only in males (Fig. 4A).

ERβ-OE preserves LV systolic and diastolic function after MI

MI surgery significantly reduced parameters of systolic and diastolic function (table 1). ERβ-OE was associated with a smaller decrease of EF, tissue Doppler S wave and with lower interventricular asynchrony in both sexes. ERβ-OE mice also showed a better preserved diastolic function after MI, as indicated by TDI E wave, E wave deceleration time, E/E' ratio and a better preservation of myocardial performance index. A genotype-surgery interaction was observed for all functional parameters. Separate analysis in each sex after MI showed a significant ERβ-OE effect on TDI S and diastolic parameters both in females and males (Fig. 4B), whereas the effect on EF was only significant in males (Fig. 4A).

Effect of ERβ-OE on hypertrophy markers after MI

MI significantly induced *NPPA* mRNA in the LV remote area compared to sham (MI vs Sham; p<0.0001). Separate analysis in each sex after MI showed that ERβ-OE significantly attenuated *NPPA* expression after MI only in male mice (supplemental Fig. 2A). *Myh6/Myh7* ratio revealed no significant change after MI (supplemental Fig. 2B). Further, measurement of signaling pathways involved in cardioprotection [17, 27], i.e. phosphorylation of AKT (p-AKT) and ERK1/2 (p-ERK1/2) showed no significant changes after MI (supplemental Fig. 2C-D).

ERβ-OE attenuates the development of cardiac fibrosis and the expression of fibrosis markers

MI induced an increase of cardiac fibrosis in the LV remote area associated with increased expression of *Col I* and *Col III* mRNA, miR21 and periostin protein (MI vs Sham; p<0.0001 for

8

all parameters). ERβ-OE was associated with lower fibrosis and reduced expression of *Col I* and *III* (ERβ-OE vs WT; p<0.05 for all three parameters). Separate analysis in each sex after MI showed that the ERβ-OE effect on fibrosis, *Col I*, and *Col III* reduction was significant only in males (Fig. 5A-5D). In addition, miR-21 expression and periostin protein were not significantly increased in male ERβ-OE compared with male WT after MI (Fig. 5E-5F). Levels of miR-24, miR-27a and miR-106a revealed no significant alteration after MI (supplemental Fig. 3). Inflammatory marker levels (Interleukin-6; tumor necrosis factor alpha; TYRO protein tyrosine kinase-binding protein and Fc receptor IgE high affinity I gamma polypeptide targeted mutation 1) were not significantly different between ERβ-OE and WT mice two weeks post-MI (data not shown).

ERβ-OE improves the expression of calcium-handling proteins
MI significantly reduced SERCA2a protein expression in the LV remote area compared to sham (p<0.0001). ERβ-OE was associated with significant higher expression of SERCA2a compared to WT (p<0.0001). Separate analysis in each sex showed that SERCA2a levels were significantly higher in female and male ERβ-OE compared to WT after MI (Fig. 6A). The ratio of phosphorylated PLN to total PLN showed no significant difference between MI groups (Fig. 6B).

Discussion

Cardioprotective effects of ERβ, particularly in females, have been reported. However, mechanistic understanding is limited and it was not possible to separate ERβ systemic effects from cardiac effects. We now show for the first time that cardiomyocyte-specific ERβ-OE led to improved survival, reduced LV remodelling, and better cardiac function in male and female mice two weeks after MI.

ERβ-OE effect on survival

Cardiomyocyte-specific ERβ-OE significantly improved survival two weeks after MI. Interestingly, we observed no LV rupture in ERβ-OE mice during the early phase after MI. This might be associated with decreased early LV remodeling and inflammation. However, our study was not an acute study and two weeks after MI we could not show any difference in inflammatory markers. The investigation of mechanisms associated with the reduction of rupture by ERβ-OE will be of high interest for future studies. In contrast to WT mice, all ERβ-OE mice survived after day 4. No heart failure associated deaths were observed in ERβ-OE animals and this can be related to reduced LV remodelling and to improved systolic and diastolic function. Long term pro-survival effects of ERβ in female mice have also been suggested by loss of function studies with increased mortality in female ERβ^{-/-} [12, 11, 13, 14], associated with an increase in heart failure markers [11]. Data from our study show improved survival after MI in females by ERβ-OE, underscoring the beneficial role of ERβ in females. However, our findings on improved survival by ERβ-OE in males are completely novel, and may reveal an interesting pathway for cardioprotection in males. In contrast to studies with systemic modulation of ERβ, our study is based on a cardiomyocyte-specific approach. We can thus exclude the contribution of systemic effects.

ERβ-OE effect on MI size, LV remodelling and cardiac function

Improved survival and reduced maladaptive remodelling in ERβ-OE mice were not related to a different MI size compared to WT. These results are in accordance with previous studies of Korte *et al.* and Pelzer *et al.* who observed no change in MI size in ERβ^{-/-} females [12, 11]. After MI, ERβ-OE in cardiomyocytes induced a smaller increase of LV enddiastolic and endsystolic volumes, and a smaller decrease of EF compared to WT. Parameters of myocardial function like TDI S and E' wave, reflecting intrinsic myocardial relaxation and contraction, showed a significantly better preservation in ERβ-OE mice. ERβ-OE was also associated with a lower increase of interventricular asynchrony. Cardiac asynchrony, due to asynchronous contraction between the right ventricle and the infarcted LV, is an important prognostic marker in patients after MI for survival, cardiac remodelling and function [20]. Diastolic parameters like E wave deceleration time and the E/E' ratio were significantly less impaired in ERβ-OE mice, indicating less increased LV filling pressures. This is in agreement with the observation of lower lung weight in ERβ-OE, suggesting attenuated HF compared to WT. Finally, the myocardial performance index, a global marker of systolic and diastolic function was significantly less increased in ERβ-OE, indicating higher global efficiency.

Although most of these functional parameters were improved in females and males by ERβ-OE, the effect on LV volumes and on EF was more pronounced in males compared to females. This difference seems to be due, at least in part, to the fact that male WT showed worse maladaptive remodelling and thus benefited most from ERβ-OE.

Molecular mechanism of ERβ induced cardioprotection

This study identified two molecular pathways by which ERβ might contribute to cardioprotection. First, we observed a lower reduction of SERCA2a protein expression in male and female ERβ-OE after MI compared to WT mice. In human and experimental heart failure a diminished Ca^{2+} uptake resulting from decreased expression/activity of SERCA2a is recognized as a hallmark of heart failure [28]. In cardiomyocytes, SERCA2a plays a central role in Ca^{2+} cycling required for both relaxation and contraction [29]. SERCA2a transports Ca^{2+} from the cytosol into the sarcoplasmic reticulum (SR), thereby contributing to the low diastolic Ca^{2+} levels required for relaxation and replenishing Ca^{2+} stores needed for the next contraction [30]. While SERCA2a homozygous knockout mice (SERCA2a^{-/-}) die early in

10

development, heterozygous SERCA2a mice (SERCA2a$^{+/-}$) showed decreased myocyte contractility and SR Ca^{2+} load, resulting to heart failure in combination with an increased hemodynamic load [31, 30]. On the other hand, a SERCA2a overexpression in the heart of transgenic mice accelerates calcium transients and cardiac relaxation resulting in higher cardiac contractility [32, 33]. In our study, a better reuptake of calcium from the cytosol to the SR via an increased expression of the calcium-ATPase during diastole might explain a better myocardial relaxation, as indicated by improved TDI E' in ERβ-OE as compared to WT mice. Increased SR calcium content due to higher SERCA2a expression might in turn explain a more important calcium release via the ryanodine receptors and an increase of the calcium transient during systole. This could contribute to better intrinsic contraction as indicated by improved TDI S and better global myocardial performance as observed in ERβ-OE males and females. Improved Ca^{2+}-cycling between SR and the cytosol might thus constitute a mechanism of cardioprotection mediated by ERβ.

Second, reduced maladaptive remodelling observed with ERβ-OE was associated with lower cardiac fibrosis and expression of fibrosis markers after MI, particularly in male mice. Post-infarct LV remodelling is due to infarct expansion but also to remodelling processes in the remote zone. While healing of the infarct zone with a firm fibrous scar is essential for chamber integrity, exaggerated fibrosis in the remote zone can lead to maladaptive remodelling, thus contributing to cardiac dysfunction [34]. Attenuated cardiac fibrosis in male ERβ-OE might be therefore one underlying reason for significantly less maladaptive remodelling and better EF (as a volume-dependent parameter). ERβ-OE in female hearts did not attenuate fibrosis after MI compared to female WT, which might be due to the fact that females develop less fibrosis compared to male WT-mice [14]. Further, Pelzer *et al.* [11] showed also no ERβ-mediated modulation of the myocardial collagen content in female ERβ$^{-/-}$ compared to WT females after MI. Sex specific antifibrotic effects of ERβ have already been described in different mouse models, e.g. pressure overload induced myocardial hypertrophy. Our recent studies showed ERβ-mediated sex-specific cardiac remodelling in a pressure overload induced mouse model and in miRNA regulation involved in cardiac fibrosis development [14, 35].

Reduced fibrosis and expression of fibrosis markers in male ERβ-OE mice may be mediated by reduction of miR-21 expression. Silencing of miR-21 in different HF models led to the suppression of cardiac fibrosis, collagen and periostin expression and attenuation of cardiac dysfunction [36-38]. ERβ-mediated down-regulation of miRNA21 has been described by us and others [35, 39] and could have contributed to antifibrotic effects in male ERβ-OE mice. These data indicate that ERβ plays an important role in the development of fibrosis in male sex after MI.

Study limitations

An overexpression model, as a gain of function model, does not exactly reflect the ERβ effect in a physiological setting. However, it may illustrate the potential effects of specific ERβ agonists on cardiomyocytes. Further studies are necessary to study the effects of ERβ in the setting of acute MI, including in particular the pathways associated with LV rupture during the early phase post-MI, which was reduced by ERβ-OE. Although our model was based on a cardiomyocyte-specific approach, we cannot exclude the involvement of other cardiac cell types. Cellular cross-talk between cardiomyocytes and fibroblasts in particular might have contributed to the observed effects on fibrosis. Further mechanistic studies are necessary to investigate the role of this cellular cross talk.

Clinical perspectives

i) The lower incidence of ischemic cardiomyopathy in premenopausal women compared to age-matched men raises the crucial question about the mechanisms of estrogen and estrogen receptor mediated cardioprotection, which is incompletely understood. In experimental models, ERβ activation has been shown to be cardioprotective, but involved cell types and mechanisms are unclear.

(ii) In the present study, cardiomyocyte-specific overexpression of ERβ in the setting of chronic MI induced improved survival in mice of both sexes and was associated with less maladaptive LV remodelling, better cardiac function and less HF development.

(iii) Overexpression of ERβ in cardiomyocytes conferred significant cardioprotective effects, which may lead to the development of therapies that selectively enhance beneficial ERβ effects in female and male hearts. Subtype-selective estrogen receptor modulators are already used in clinical practice or are currently tested for the treatment of breast cancer and osteoporosis [40] and may also be of interest in the treatment of cardiac diseases.

Author contribution statement
Iris Schuster: performing experiments, data acquisition and analysis, manuscript writing.

Shokoufeh Mahmoodzadeh: study design and planning, performing experiments, data acquisition and analysis, manuscript writing.

Elke Dworatzek: performing experiments, data acquisition and analysis, manuscript writing.

Frédéric Jaisser: Generation of monotransgenic ERβ and monotransgenic tTA mice; contributed to discussion and critical revision of the manuscript.

Smail Messaoudi: Generation of monotransgenic ERβ and monotransgenic tTA mice; contributed to discussion and critical revision of the manuscript.

Ingo Morano: cardiomyocyte isolation, evaluation of cardiomyocyte size; contributed to discussion and critical revision of the manuscript.

Vera Regitz-Zagrosek: study design and planning and manuscript writing.

References

1. Piro M, Della Bona R, Abbate A, Biasucci LM, Crea F. Sex-related differences in myocardial remodeling. Journal of the American College of Cardiology. 2010;55(11):1057-65. doi:10.1016/j.jacc.2009.09.065.

2. Dunlay SM, Roger VL. Gender differences in the pathophysiology, clinical presentation, and outcomes of ischemic heart failure. Current heart failure reports. 2012;9(4):267-76. doi:10.1007/s11897-012-0107-7.

3. O'Meara E, Clayton T, McEntegart MB, McMurray JJ, Pina IL, Granger CB et al. Sex differences in clinical characteristics and prognosis in a broad spectrum of patients with heart failure: results of the Candesartan in Heart failure: Assessment of Reduction in Mortality and morbidity (CHARM) program. Circulation. 2007;115(24):3111-20. doi:10.1161/CIRCULATIONAHA.106.673442.

4. Cavasin MA, Tao Z, Menon S, Yang XP. Gender differences in cardiac function during early remodeling after acute myocardial infarction in mice. Life sciences. 2004;75(18):2181-92. doi:10.1016/j.lfs.2004.04.024.

5. Grohe C, Kahlert S, Lobbert K, Stimpel M, Karas RH, Vetter H et al. Cardiac myocytes and fibroblasts contain functional estrogen receptors. FEBS letters. 1997;416(1):107-12.

6. Mahmoodzadeh S, Eder S, Nordmeyer J, Ehler E, Huber O, Martus P et al. Estrogen receptor alpha up-regulation and redistribution in human heart failure. FASEB journal : official publication of the Federation of American Societies for Experimental Biology. 2006;20(7):926-34. doi:10.1096/fj.05-5148com.

7. Nordmeyer J, Eder S, Mahmoodzadeh S, Martus P, Fielitz J, Bass J et al. Upregulation of myocardial estrogen receptors in human aortic stenosis. Circulation. 2004;110(20):3270-5. doi:10.1161/01.CIR.0000147610.41984.E8.

8. Mahmoodzadeh S, Dworatzek E, Fritschka S, Pham TH, Regitz-Zagrosek V. 17beta-Estradiol inhibits matrix metalloproteinase-2 transcription via MAP kinase in fibroblasts. Cardiovascular research. 2010;85(4):719-28. doi:10.1093/cvr/cvp350.

9. Mendelsohn ME. Protective effects of estrogen on the cardiovascular system. The American journal of cardiology. 2002;89(12A):12E-7E; discussion 7E-8E.

10. Pedram A, Razandi M, Aitkenhead M, Hughes CC, Levin ER. Integration of the non-genomic and genomic actions of estrogen. Membrane-initiated signaling by steroid to transcription and cell biology. The Journal of biological chemistry. 2002;277(52):50768-75. doi:10.1074/jbc.M210106200.

11. Pelzer T, Loza PA, Hu K, Bayer B, Dienesch C, Calvillo L et al. Increased mortality and aggravation of heart failure in estrogen receptor-beta knockout mice after myocardial infarction. Circulation. 2005;111(12):1492-8. doi:10.1161/01.CIR.0000159262.18512.46.

12. Korte T, Fuchs M, Arkudas A, Geertz S, Meyer R, Gardiwal A et al. Female mice lacking estrogen receptor beta display prolonged ventricular repolarization and reduced ventricular automaticity after myocardial infarction. Circulation. 2005;111(18):2282-90. doi:10.1161/01.CIR.0000164262.08004.BB.

13. Babiker FA, Lips DJ, Delvaux E, Zandberg P, Janssen BJ, Prinzen F et al. Oestrogen modulates cardiac ischaemic remodelling through oestrogen receptor-specific mechanisms. Acta physiologica. 2007;189(1):23-31. doi:10.1111/j.1748-1716.2006.01633.x.

14. Fliegner D, Schubert C, Penkalla A, Witt H, Kararigas G, Dworatzek E et al. Female sex and estrogen receptor-beta attenuate cardiac remodeling and apoptosis in pressure overload. American journal of physiology Regulatory, integrative and comparative physiology. 2010;298(6):R1597-606. doi:10.1152/ajpregu.00825.2009.

15. Bernardo BC, Weeks KL, Pretorius L, McMullen JR. Molecular distinction between physiological and pathological cardiac hypertrophy: experimental findings and therapeutic strategies. Pharmacology & therapeutics. 2010;128(1):191-227. doi:10.1016/j.pharmthera.2010.04.005.

16. Weeks KL, Gao X, Du XJ, Boey EJ, Matsumoto A, Bernardo BC et al. Phosphoinositide 3-kinase p110alpha is a master regulator of exercise-induced cardioprotection and PI3K gene therapy rescues cardiac dysfunction. Circulation Heart failure. 2012;5(4):523-34. doi:10.1161/CIRCHEARTFAILURE.112.966622.

17. McMullen JR, Amirahmadi F, Woodcock EA, Schinke-Braun M, Bouwman RD, Hewitt KA et al. Protective effects of exercise and phosphoinositide 3-kinase(p110alpha) signaling in dilated and hypertrophic cardiomyopathy. Proceedings of the National Academy of Sciences of the United States of America. 2007;104(2):612-7. doi:10.1073/pnas.0606663104.

18. Dworatzek E, Mahmoodzadeh S, Schubert C, Westphal C, Leber J, Kusch A et al. Sex differences in exercise-induced physiological myocardial hypertrophy are modulated by oestrogen receptor beta. Cardiovascular research. 2014;102(3):418-28. doi:10.1093/cvr/cvu065.

19. Wang M, Wang Y, Weil B, Abarbanell A, Herrmann J, Tan J et al. Estrogen receptor beta mediates increased activation of PI3K/Akt signaling and improved myocardial function in female hearts following acute ischemia. American journal of physiology Regulatory, integrative and comparative physiology. 2009;296(4):R972-8. doi:10.1152/ajpregu.00045.2009.

20. Cleland JG, Daubert JC, Erdmann E, Freemantle N, Gras D, Kappenberger L et al. The effect of cardiac resynchronization on morbidity and mortality in heart failure. The New England journal of medicine. 2005;352(15):1539-49. doi:10.1056/NEJMoa050496.

21. Lang RM, Badano LP, Mor-Avi V, Afilalo J, Armstrong A, Ernande L et al. Recommendations for cardiac chamber quantification by echocardiography in adults: an update from the American Society of Echocardiography and the European Association of Cardiovascular Imaging. European heart journal cardiovascular Imaging. 2015;16(3):233-70. doi:10.1093/ehjci/jev014.

22. Bauer M, Cheng S, Jain M, Ngoy S, Theodoropoulos C, Trujillo A et al. Echocardiographic speckle-tracking based strain imaging for rapid cardiovascular phenotyping in mice. Circulation research. 2011;108(8):908-16. doi:10.1161/CIRCRESAHA.110.239574.

23. Ram R, Mickelsen DM, Theodoropoulos C, Blaxall BC. New approaches in small animal echocardiography: imaging the sounds of silence. American journal of physiology Heart and circulatory physiology. 2011;301(5):H1765-80. doi:10.1152/ajpheart.00559.2011.

24. Kanno S, Lerner DL, Schuessler RB, Betsuyaku T, Yamada KA, Saffitz JE et al. Echocardiographic evaluation of ventricular remodeling in a mouse model of myocardial infarction. Journal of the American Society of Echocardiography : official publication of the American Society of Echocardiography. 2002;15(6):601-9.

25. Benavides-Vallve C, Corbacho D, Iglesias-Garcia O, Pelacho B, Albiasu E, Castano S et al. New strategies for echocardiographic evaluation of left ventricular function in a mouse model of long-term myocardial infarction. PloS one. 2012;7(7):e41691. doi:10.1371/journal.pone.0041691.

26. Mahmoodzadeh S, Leber J, Zhang X, Jaisser F, Messaoudi S, Morano I et al. Cardiomyocyte-specific Estrogen Receptor Alpha Increases Angiogenesis, Lymphangiogenesis and Reduces Fibrosis in the Female Mouse Heart Post-Myocardial Infarction. Journal of cell science & therapy. 2014;5(1):153. doi:10.4172/2157-7013.1000153.

27. Lips DJ, Bueno OF, Wilkins BJ, Purcell NH, Kaiser RA, Lorenz JN et al. MEK1-ERK2 signaling pathway protects myocardium from ischemic injury in vivo. Circulation. 2004;109(16):1938-41. doi:10.1161/01.CIR.0000127126.73759.23.

28. Schwartz RJ, Yeh ET. Weighing in on heart failure: the role of SERCA2a SUMOylation. Circulation research. 2012;110(2):198-9. doi:10.1161/RES.0b013e318246f187.

29. Kranias EG, Hajjar RJ. Modulation of cardiac contractility by the phospholamban/SERCA2a regulatome. Circulation research. 2012;110(12):1646-60. doi:10.1161/CIRCRESAHA.111.259754.

30. Periasamy M, Reed TD, Liu LH, Ji Y, Loukianov E, Paul RJ et al. Impaired cardiac performance in heterozygous mice with a null mutation in the sarco(endo)plasmic reticulum Ca2+-ATPase isoform 2 (SERCA2) gene. The Journal of biological chemistry. 1999;274(4):2556-62.

31. Schultz Jel J, Glascock BJ, Witt SA, Nieman ML, Nattamai KJ, Liu LH et al. Accelerated onset of heart failure in mice during pressure overload with chronically decreased SERCA2 calcium pump activity. American journal of physiology Heart and circulatory physiology. 2004;286(3):H1146-53. doi:10.1152/ajpheart.00720.2003.

32. He H, Giordano FJ, Hilal-Dandan R, Choi DJ, Rockman HA, McDonough PM et al. Overexpression of the rat sarcoplasmic reticulum Ca2+ ATPase gene in the heart of transgenic mice accelerates calcium transients and cardiac relaxation. The Journal of clinical investigation. 1997;100(2):380-9. doi:10.1172/JCI119544.

33. Baker DL, Hashimoto K, Grupp IL, Ji Y, Reed T, Loukianov E et al. Targeted overexpression of the sarcoplasmic reticulum Ca2+-ATPase increases cardiac contractility in transgenic mouse hearts. Circulation research. 1998;83(12):1205-14.

34. Kong P, Christia P, Frangogiannis NG. The pathogenesis of cardiac fibrosis. Cellular and molecular life sciences : CMLS. 2014;71(4):549-74. doi:10.1007/s00018-013-1349-6.

35. Queiros AM, Eschen C, Fliegner D, Kararigas G, Dworatzek E, Westphal C et al. Sex- and estrogen-dependent regulation of a miRNA network in the healthy and hypertrophied heart. International journal of cardiology. 2013;169(5):331-8. doi:10.1016/j.ijcard.2013.09.002.

36. Thum T, Gross C, Fiedler J, Fischer T, Kissler S, Bussen M et al. MicroRNA-21 contributes to myocardial disease by stimulating MAP kinase signalling in fibroblasts. Nature. 2008;456(7224):980-4. doi:10.1038/nature07511.

37. Adam O, Lohfelm B, Thum T, Gupta SK, Puhl SL, Schafers HJ et al. Role of miR-21 in the pathogenesis of atrial fibrosis. Basic research in cardiology. 2012;107(5):278. doi:10.1007/s00395-012-0278-0.

38. Cardin S, Guasch E, Luo X, Naud P, Le Quang K, Shi Y et al. Role for MicroRNA-21 in atrial profibrillatory fibrotic remodeling associated with experimental postinfarction heart failure. Circulation Arrhythmia and electrophysiology. 2012;5(5):1027-35. doi:10.1161/CIRCEP.112.973214.

39. Paris O, Ferraro L, Grober OM, Ravo M, De Filippo MR, Giurato G et al. Direct regulation of microRNA biogenesis and expression by estrogen receptor beta in hormone-responsive breast cancer. Oncogene. 2012;31(38):4196-206. doi:10.1038/onc.2011.583.

40. Nilsson S, Koehler KF, Gustafsson JA. Development of subtype-selective oestrogen receptor-based therapeutics. Nature reviews Drug discovery. 2011;10(10):778-92. doi:10.1038/nrd3551.

Tables

Table 1: Left ventricular echocardiographic data and organ weight two weeks after myocardial infarction or sham surgery in female and male wild type and ERβ-OE mice

	Female WT Sham (n=17)	Female WT MI (n=13)	Male WT Sham (n=18)	Male WT MI (n=14)	Female ERβOE Sham (n=18)	Female ERβOE MI (n=18)	Male ERβOE Sham (n=15)	Male ERβOE MI (n=10)	MI effect	Sex effect	ERβ effect	interaction
Heart rate (bpm)	460±3	479±4	457±3	480±5	454±5	479±4	457±4	476±3	<0.0001	NS	NS	
MI size (%)		47±1	-	51±2	-	45±1	-	47±3	-	NS	NS	
LV Morphology												
Mean wall thickness (mm)	0.65±0.01	0.56±0.01	0.66±0.01	0.55±0.02	0.67±0.01	0.56±0.02	0.68±0.01	0.57±0.02	<0.0001	NS	NS	
LVEDV (µl)	53±2	77±2	67±2	110±9	48±1	72±5	64±2	83±4	<0.0001	<0.0001	<0.001	*○
LVESV (µl)	18±1	52±3	24±1	81±9	16±1	47±5	21±2	51±4	<0.0001	<0.001	<0.001	*○
Systolic function												
Ejection fraction (%)	65±1	34±2	66±2	26±2	67±1	39±2	66±2	40±3	<0.0001	NS	0.01	*○
TDI S (cm.s^{-1})	24±1	16±1	26±1	15±1	25±1	20±1	26±1	20±1	<0.0001	NS	0.01	*
Asynchrony Index (ms)	0.6±0.1	3.4±0.3	0.7±0.1	5.0±0.9	0.6±0.1	2.0±0.3	0.8±0.2	3.1±0.2	<0.0001	<0.01	<0.01	*
Diastolic function												
EWDT time (ms)	28±1	17±1	30±2	13±1	30±1	22±1	30±2	19±2	<0.0001	NS	0.01	*
TDI E' (cm.s^{-1})	33±1	23±1	35±1	20±1	34±1	28±1	33±1	28±1	<0.0001	NS	0.01	*
E/E' ratio	26±1	36±2	25±1	37±2	25±2	29±2	26±1	27±1	<0.0001	NS	<0.01	*
Myocardial performance index	0.27±0.02	0.74±0.04	0.29±0.03	0.90±0.10	0.31±0.02	0.55±0.05	0.29±0.02	0.69±0.06	<0.0001	NS	<0.05	*
Organ weight (µg/mm) Heart weight/TL	6.5±0.02	9.2±0.04	8.5±0.03	11.7±0.10	6.9±0.02	8.4±0.05	8.6±02	9.9±0.06	<0.0001	<0.0001	<0.01	*

16

Lung weight/TL	8.0±0.1	9.5±0.2	8.5±0.2	10.7±0.5	8.2±0.1	8.6±0.2	8.5±0.2	9.8±0.4	<0.0001	<0.0001	<0.05	*
Liver weight/TL	59±3	66±2	72±2	79±4	60±2	61±1	73±3	75±3	NS	<0.0001	<0.05	
Uterus weight/TL	5.0±0.6	5.4±0.5	-	-	5.2±0.4	5.3±0.5	-	-	NS	<0.0001	<0.05	

Data are presented as mean±SEM. ANOVA analysis for surgery (MI vs sham), genotype (ERβ-OE vs WT) and sex effect (male vs female).
Interaction analysis between factors: Genotype-operation interaction* and sex-genotype-operation interaction° p<0.05.
LVEDV: left ventricular enddiastolic volume; LVESV: left ventricular endsystolic volume; TL: tibia length; TDI S: tissue Doppler systolic S wave at the septal border of the mitral annulus; TDI E': tissue Doppler diastolic E' wave at the septal border of the mitral annulus; EWDT: E wave deceleration time.

17

Figure legends

Figure 1: Echocardiographic MI size determination. (A) Example of MI size determination from the long axis view and (B) from the short axis view, (C) Correlation between MI size determination from long and short axis view.

Figure 2. Characterization of ERβ-OE mice. (A) Diastolic cardiomyocyte length and width are not different between ERβ-OE and WT-mice. Data are mean ± SEM for 100-300 cells/group, (B) ERβ protein level is higher in LV tissue of female and male ERβ-OE compared to WT-mice (n≥7/group), 2-way ANOVA: p<0.01 for both groups (genotype effect: ERβ-OE vs. WT), (C) Immunofluorescence of ERβ (green) in cardiomyocytes of ERβ-OE and WT. Nuclei are in blue (DAPI). 20x magnification, scale bar: 250μm, (D) ERα protein level is not changed by ERβ-OE overexpression. Tubulin was used as control. Bars are represented as mean ± SEM (n≥7/group).

Figure 3. Survival curves of ERβ-OE and WT-mice. Kaplan-Meier curves of female ERβ-OE (dashed grey line; n=18), male ERβ-OE (dashed black line; n=12), female WT (continuous grey line; n=17) and male WT (continuous black line; n=24). Genotype effect: ERβOE vs WT: p=0.008.

Figure 4. Effect of ERβ-OE on LV morphology and function in MI groups. (A) Effect on LV volumes and ejection fraction (EF). (B) Effect on parameters of intrinsic myocardial systolic and diastolic function (TDI S, TDI E, E/E' ratio, E wave deceleration time). 2-way ANOVA for sex and genotype in MI groups: *p<0.05, **p<0.01, and ***p<0.001. Data are expressed as mean ± SEM of n≥12 per group.

Figure 5. ERβ-OE attenuates fibrosis in male mice. (A) Representative images of Sirius red-stained LV tissues from female and male WT and ERβ-OE mice after MI (remote area). 10x magnification, scale bar: 200μm. (B) Percentage of fibrosis in LV remote area. (C) Col I, (D) Col III mRNA, (E) miR-21 expression, (F) Periostin protein. For all analyses: 2-way ANOVA: MI-effect independent of genotype *p<0.05 and ***p<0.001; genotype effect independent of sex §p<0.05, §§p<0.01 and §§§p<0.001. Data are mean ± SEM of n≥8/group.
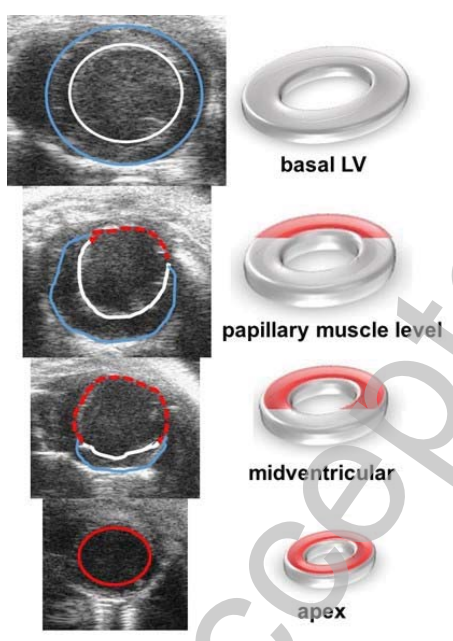
Figure 6. ERβ-OE improves the expression of calcium-handling protein. (A) SERCA2a and (B) p-PLN/PLN protein expression. 2-way ANOVA: MI-effect independent of genotype **p<0.01; and genotype effect independent of sex §p<0.05. Data are mean ± SEM of n≥8/group.

Figure 1

A

B

basal LV

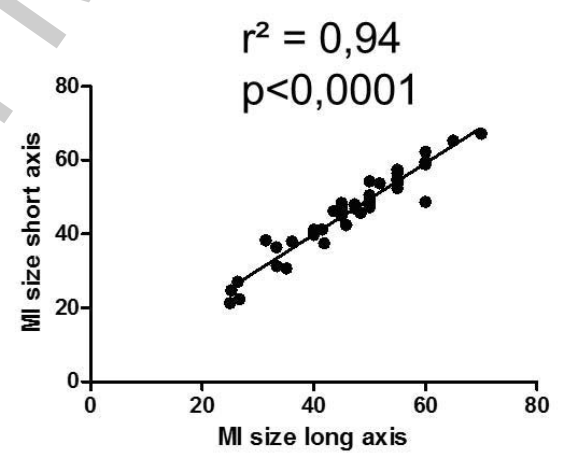papillary muscle level

midventricular

apex

C

Figure 2

A

B

56 kDa — ERβ
50 kDa — α-Tubulin

C

ERβ   Dapi

D

66 kDa — ERα
50 kDa — α-Tubulin
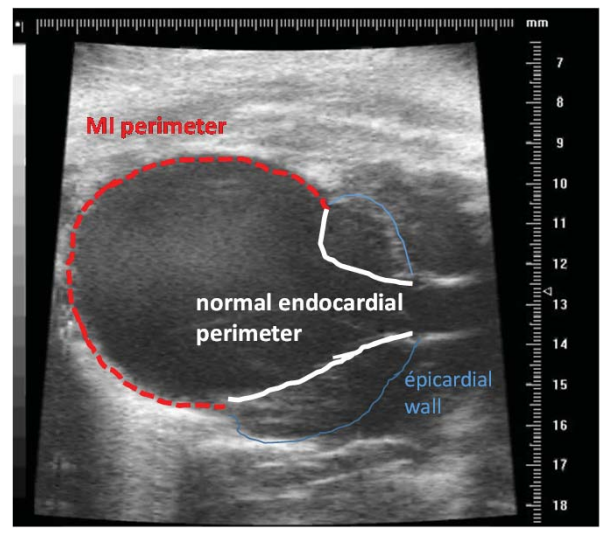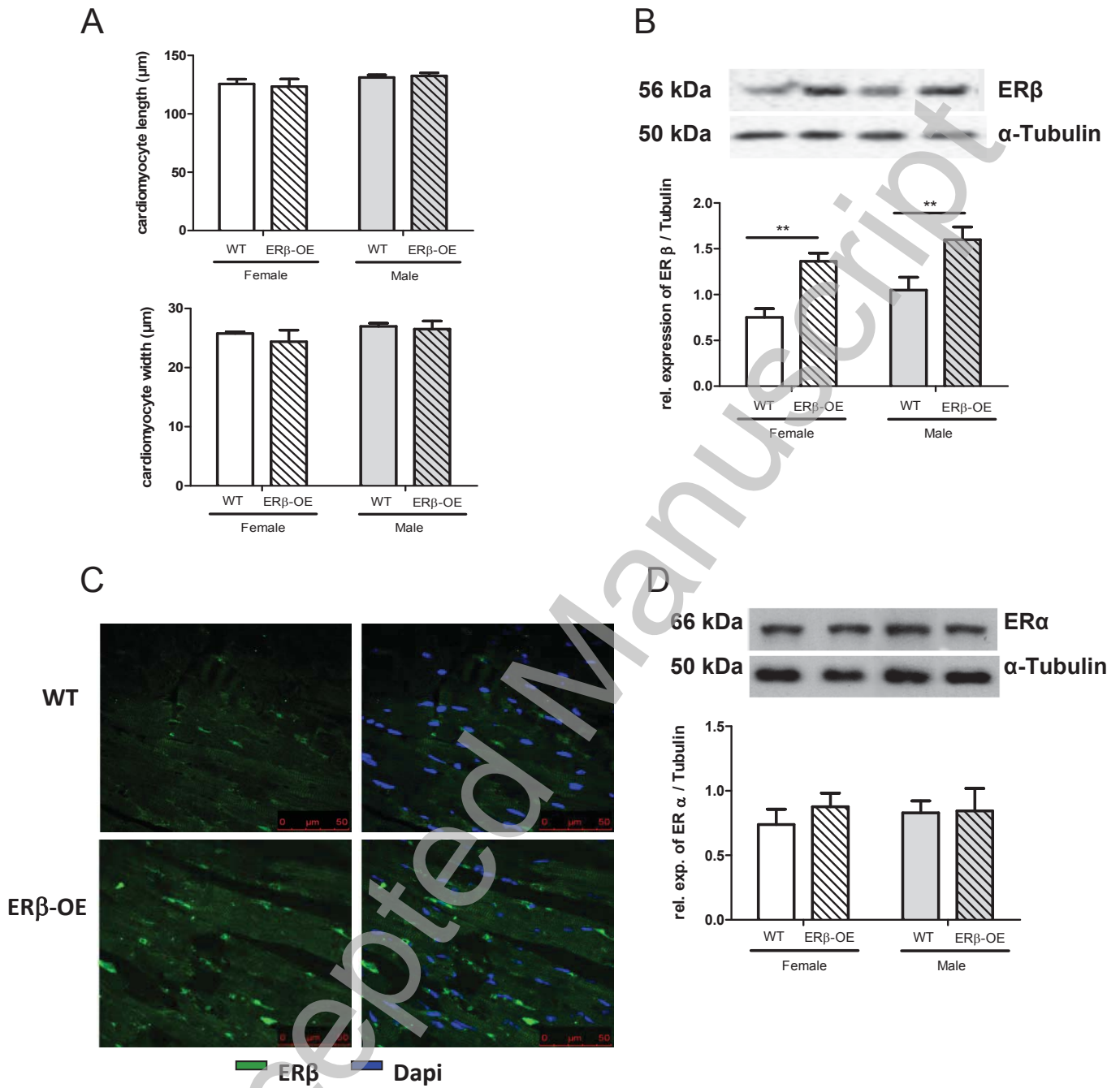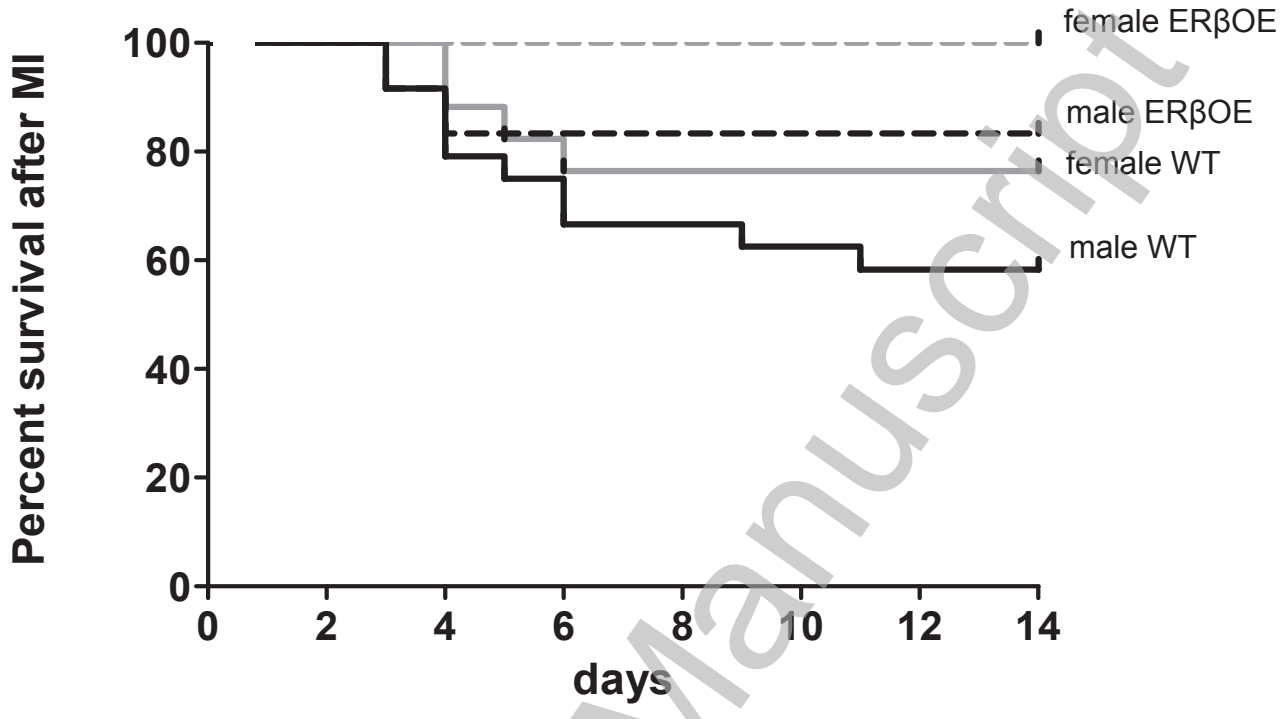
Figure 3

Figure 4

A

B

Figure 5

Figure 6

A

B